Catal Lett (2008) 125:83–89
DOI 10.1007/s10562-008-9515-4

Skeletal Isomerization of *n*-Pentane over Platinum-Promoted Tungstophosphoric Acid Supported on MCM-41

Yuandong Xu · Yanxing Qi · Gongxuan Lu · Shuben Li

Received: 20 March 2008 / Accepted: 5 May 2008 / Published online: 17 June 2008

Abstract Skeletal isomerization of *n*-pentane in the presence of hydrogen has been studied over Pt-promoted $H_3PW_{12}O_{40}$ (TPA)/MCM-41 bifunctional catalyst. A series of solid acid catalysts with different loading amount of TPA and Pt were prepared and characterized by XRD, FT-IR and XPS. The optimal catalytic activity of Pt-TPA/MCM-41 was observed with 2% Pt and 30% TPA. According to the cracked products distribution, this is typical of a monomolecular bifunctional metal-acid mechanism. Further, catalysts with different combination of noble metals (Pt, Pd and Ru), heteropoly acids (HPAs) (TPA, tungstosilicic acid (TSA), and molybdophosphoric acid (MPA)) and supports (MCM-41, SBA-1 and SiO_2) were also synthesized and their catalytic performances were compared.

Keywords Skeletal isomerization · *n*-Pentane · Tungstophosphoric acid · MCM-41

1 Introduction

Skeletal isomerization of *n*-pentane and *n*-hexane which are the main components of the light straight run (LSR) gasoline fraction to mono- or di-branched molecule is an important catalytic process in the petroleum industry, since the branched alkanes increase the octane number of the gasoline pool. In this way the research octane number (RON) of the LSR increases from ~64 to ~80 [1]. Currently, the commercial catalysts used for carrying out this isomerization reaction are chlorinated alumina containing Pt and Pt/H-mordenite. Although the former has a low reaction temperature of 423 K it is sensitive to water and sulfur even in concentrations as low as 10 ppm and also leads to environmental problems due to the utilization of halogen. On the other hand, the latter on which the acid strength is weaker than that of chlorinated alumina was carried out at a significantly higher temperature of 523 K with the corresponding 2-point RON penalty [2].

In the past few years, solid acid materials, such as sulfated zirconia [2–4], tungstated zirconia [5–7] and HPAs-based materials [8–10], exhibiting higher acid strength than that of conventional inorganic liquid acid and zeolites, were applied to the skeletal isomerization of light alkanes. Among them, systems based on HPAs are the most promising. HPAs and their salts have strong acidity and can activate alkanes via the formation of carbocations. In this family TPA is the strongest acid and more often used for various acid-catalyzed reactions such as alkylation, esterification and acylation, as summarized in review article [11]. However, a significant drawback of the bulk TPA system is the low surface area that is usually less than 10 m^2/g. Though the TPA salts are widely investigated for the isomerization of *n*-alkanes [12–16], the supported systems especially the mesoporous materials used as supports are studied inadequately. Recently, Miyaji et al. [8] demonstrated that a bifunctional heteropoly catalyst, Pd-TSA/SiO_2, was highly active and selective for skeletal isomerization of *n*-pentane. Later on, the same research group investigated the isomerization of *n*-heptane over the same type catalyst [9]. At the

Y. Xu · Y. Qi (✉) · G. Lu (✉) · S. Li
State Key Laboratory for Oxo Synthesis and Selective Oxidation, Lanzhou Institute of Chemical Physics, Chinese Academy of Sciences, Lanzhou 730000, People's Republic of China
e-mail: qiyx@lzb.ac.cn

G. Lu
e-mail: gxlu@lzb.ac.cn

Y. Xu
The Graduate University of the Chinese Academy of Sciences, Beijing 10039, People's Republic of China

same time, Ivanov et al. [10] reported that Pt-promoted Keggin and Dawson TPA supported on zirconia.

Since the discovery of mesoporous silica molecular sieves with pore diameters in the 2.0–10.0 nm range of M41S family by Mobil [17], many mesoporous solids with controlled pore size and morphology have been synthesized. Among this family, MCM-41 is the most widely used mesoporous materials, its surface area (>1,000 m^2/g), thermal stability (ca. 1173 K), and pore size (1.5–8 nm) [17, 18]. So far, lots of articles have reported the MCM-41 based catalysts. HPAs supported on MCM-41 have also been tested for many reactions. However, to our knowledge, the reports published on TPA supported over MCM-41 used for *n*-alkanes skeletal isomerization were inadequate [19, 20]. In the present study, we have investigated pure siliceous MCM-41 loaded with various amount of TPA and Pt for isomerization of *n*-pentane. The reaction activities of catalysts with different combination of noble metals, HPAs and supports were also compared.

2 Experimental

Pure siliceous MCM-41 and SBA-1 were synthesized according to the method reported by Qian et al. [21] and Ji et al. [22], respectively. Pt-free catalysts were prepared from an aqueous solution of TPA and support by wet impregnation. Support in powder was dispersed in the TPA solution under vigorous stirring at room temperature for 70 min. After the solvent was removed with water bath the solid was dried in air overnight at 373 K. The process was followed by calcination in air at 573 K for 5 h. Pt-containing catalysts were prepared with the same procedure as above except that before impregnation the chloroplatinic acid solution was firstly mixed with the TPA solution. Here, the mass percentage of Pt and TPA were calculated as follows:

$$\text{Weight percent of Pt} = \text{massof Pt}/\left(\text{mass of TPA} + \text{mass of support}\right)$$

$$\text{Weight percent of TPA} = \text{mass of TPA}/\left(\text{mass of TPA} + \text{mass of support}\right)$$

The X-ray diffraction spectra measurements were performed on a Philips Xpert MPD instrument using Cu Kα radiation in the scanning angle range of 10–90° at a scanning rate of 4°/min at 40 mA and 50 kV. FT-IR spectroscopy was carried out on a Bruker IFS 120 FT-IR spectrometer using ca. 0.5 mm KBr pellets containing 2.5% sample. X-ray photoelectron spectroscopy was carried out using a VG ESCALAB 210 electron spectrometer with Mg Kα radiation.

The catalytic reaction of *n*-pentane isomerization was performed in a fixed-bed continuous flow quartz reactor (i.d. 8 mm) at atmospheric pressure. The catalysts were pelletized and sized to 20–60 mesh. Approximately 0.5 g of the catalyst was loaded into the reactor and pretreated in dried hydrogen at 473 K for 90 min. Then the hydrogen was replaced by the reaction mixture and the skeletal isomerization reaction was carried out at 473 K on a time stream of 120 min. The reaction feed was a mixture of *n*-pentane, hydrogen and nitrogen with the flow rates of 0.62, 2 and 10 mL/min, respectively. The reaction mixture flowed through the catalyst bed at an *n*-pentane weight hourly space velocity (WHSV) of 0.24 h^{-1}. The reaction products were analyzed on-line with a GC 7890 gas chromatograph equipped with an Al_2O_3/KCl plot capillary column (30 m × 0.32 mm) and a flame ionization detector.

3 Results and Discussion

XRD investigation can give us direct information about the form of the tested samples. Figure 1 illustrates the small-angle XRD patterns of the mesoporous support materials. After removal of the template, MCM-41 retains the long-range hexagonal order and exhibits three distinct diffraction peaks that can be indexed as (100), (110) and (200) [23]. According to the wide angle XRD patterns in Fig. 2, the reflection patterns of TPA corresponding to different loading amount of TPA on MCM-41 are weak and not to be observed when the TPA loading amount is less than 35%. Nevertheless, the XRD pattern of TPA with 35% content of TPA on MCM-41 exhibits apparent strong characteristic bulk TPA diffraction peaks at $2(\theta) = 10.3$ and 25.4 [24]. Because the XRD pattern is related to whether a separate detectable crystal phase exists or not,

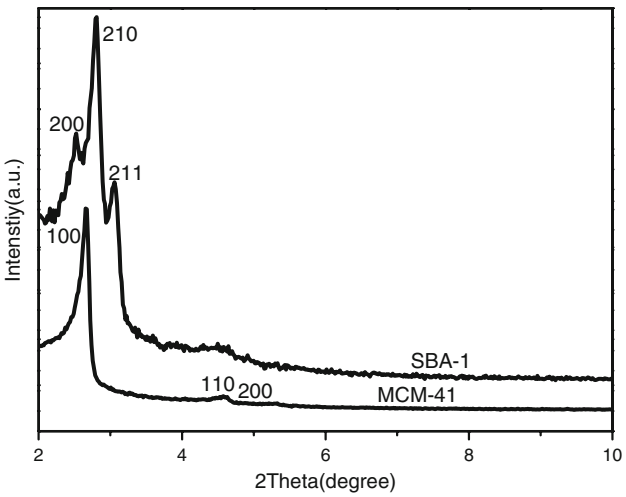

Fig. 1 XRD patterns of MCM-41 and SBA-1

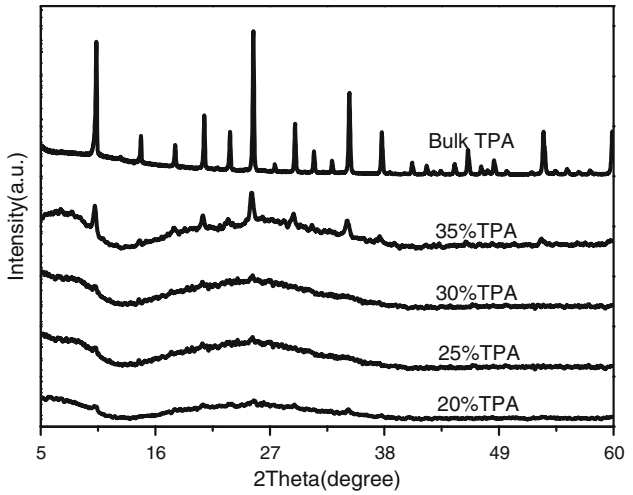

Fig. 2 XRD patterns of bulk TPA and 2% Pt/MCM-41 with different loading amount of TPA

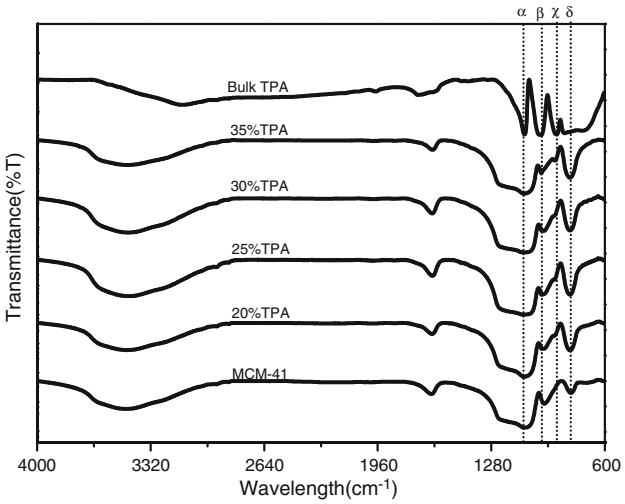

Fig. 3 FT-IR spectra of MCM-41, bulk TPA and 2% Pt/MCM-41 with different loading amount of TPA

the above XRD data illustrate that the impregnated TPA species is finely dispersed on the surfaces of MCM-41 substrate at the TPA loading amount as high as 30%. If the loading amount is further increased, part of the impregnated TPA will aggregate into a separate crystal phase. The XRD pattern of another mesoporous molecular sieve of SBA-1 which is also shown in Fig. 1 demonstrates three sharp XRD diffraction peaks in the region of $2\theta = 1.5$–3°, which are indexed to the (200), (210) and (211) diffraction peaks, respectively [25].

The form and microcosmic chemical environment therein of the detected species are more related to a framework of FT-IR spectrum resulting from bond vibrations than to the phase in which the detected molecule or material exists. FT-IR is thus a suitable method for the structural characterization of polyanions. In order to determine the state of the TPA species impregnated on MCM-41 substrate, the framework of FT-IR spectra of the samples were further investigated (see Fig. 3). From the FT-IR spectrum of MCM-41, a broad band around 3425 cm^{-1} assigned to OH stretching vibration of MCM-41, which could be associated to Si–OH and water vibration, appeared. Despite that, another broad band around 1300–1000 cm^{-1} of MCM-41 is assigned to asymmetric stretching mode of Si–O–Si. The band at 801 cm^{-1} and 966 cm^{-1} are due to the symmetric stretching vibration of rocking mode of Si–O–Si bond and the presence of Si–OH symmetric stretching vibration, respectively. There are four main absorption peaks, which were observed at 1082 cm^{-1} (α) band for P–O, 983 cm^{-1} (β) band for W = O and both 895 cm^{-1} (χ) and 810 cm^{-1} (δ) bands for W–O–W [26] ascribing to asymmetric bond stretching vibration, assigned for pure bulk TPA. Form the FT-IR spectrum of MCM-41, it is clearly that there are no peak present around 900 cm^{-1}. However, a weak band at $\sim$900 cm^{-1} appears even for the lowest loading amount of 20% TPA. This band is enhanced with the increase of TPA loading amount and the same development trend occurred to the band at 801 cm^{-1}. Nevertheless, the absorption peaks of the catalyst samples with different loading amount of TPA at bands 1082 and 983 cm^{-1} have no obvious distinction compared with each other and those of MCM-41 owing to the overlapping of TPA bands with that of MCM-41. However, as shown in Fig. 2, there are no obvious XRD patterns present for the catalysts with TPA loading amount less than 35%, indicating that these impregnated TPA species exist in a discrete state with Keggin structure. These TPA species in such state became a separate phase when the loading amount was increased to 35%. Therefore, the main TPA diffraction peaks were detected.

The information about surface chemical composition and element oxidation states of materials can be obtained from XPS measurement. The surface chemical oxidation states of Pt in 2% Pt-30% TPA/MCM-41, which was reduced in 30 mL/min hydrogen flow at 473 K for 90 min, were determined by XPS. Figure 4 shows the regional Pt4f spectra. The Pt4f spectrum obtained directly from XPS shows a doublet energy band, a low-energy band at 73.2 eV and a high-energy band at 75.2 eV. To identify different oxidation states of Pt, the spectrum was de-convoluted into two pairs of peaks at 71.1 and 74.4 eV and at 72.2 and 75.8 eV [27], respectively. These two pairs of peaks indicates that Pt(IV) in platinum precursor was reduced into two different oxidation states, Pt(0) and Pt(II). It demonstrates that Pt can not be completely reduced to zero valence under the reduction conditions. As we all know, usually improving the reduction temperature or prolonging the reduction time or increasing the reduction

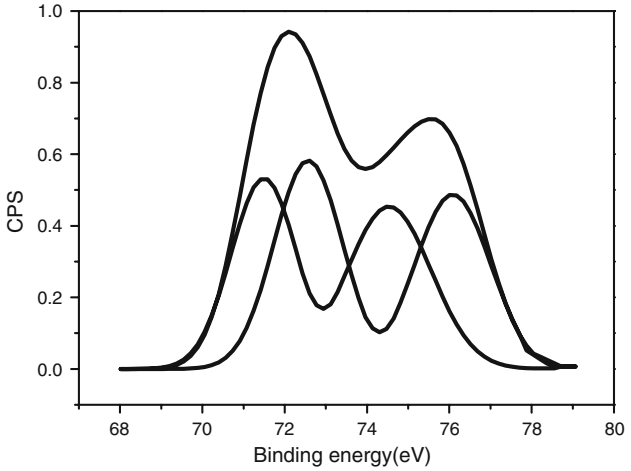

Fig. 4 Regional XPS spectra of Pt4f in 2% Pt-30% TPA/MCM-41 after reduction in hydrogen flow

gas velocity are all avail for the depth reduction of metals. In order to verify whether further reduction is good for the catalytic performance or not the above measures were taken, respectively, and their effects on the catalytic activities are illustrated in Fig. 5. It can be seen from Fig. 5a and b that improving the reduction temperature from 473 K to 523 K and increasing the reduction time from 90 to 120 min both apparently decreased the conversion of *n*-pentane while the selectivity remained nearly the same. Figure 5c demonstrates the effect of reduction gas velocity on the conversion and selectivity. Obviously, the catalyst reduced by 30 mL/min of reduction gas velocity presented more stable activity and higher selectivity. Based on the experimental results no measure of the above description could enhance the catalytic performance. It is suggested that depth reduction of Pt is disadvantageous for the isomerization of *n*-pentane. Nevertheless, it can't be exclude that, during the depth reduction the protonic density of the catalyst may be damaged.

The *n*-pentane isomerization over Pt/MCM-41, TPA/MCM-41 and Pt-TPA/MCM-41 were compared (see Fig. 6). The Pt-free TPA/MCM-41 and the TPA-free Pt/MCM-41 catalysts both exhibited very low activities less than 10% conversion. It was different from the results reported in [19, 20], in which the conversions of n-butane and n-hexane on TPA/MCM-41 were ca. 30% and ca. 65%, respectively. Nevertheless, the TPA loading were very high (ca. 75%) and the isomerization reactions were performed under high pressures according to their application examples. When Pt and TPA were together added forming the Pt-TPA/MCM-41 catalyst the conversion was significantly enhanced and nearly attained to 60%. The comparison results demonstrated that the higher activity of the catalyst originated from the synergistic effect of Pt and TPA. Pt activates alkanes to form the corresponding olefins, which

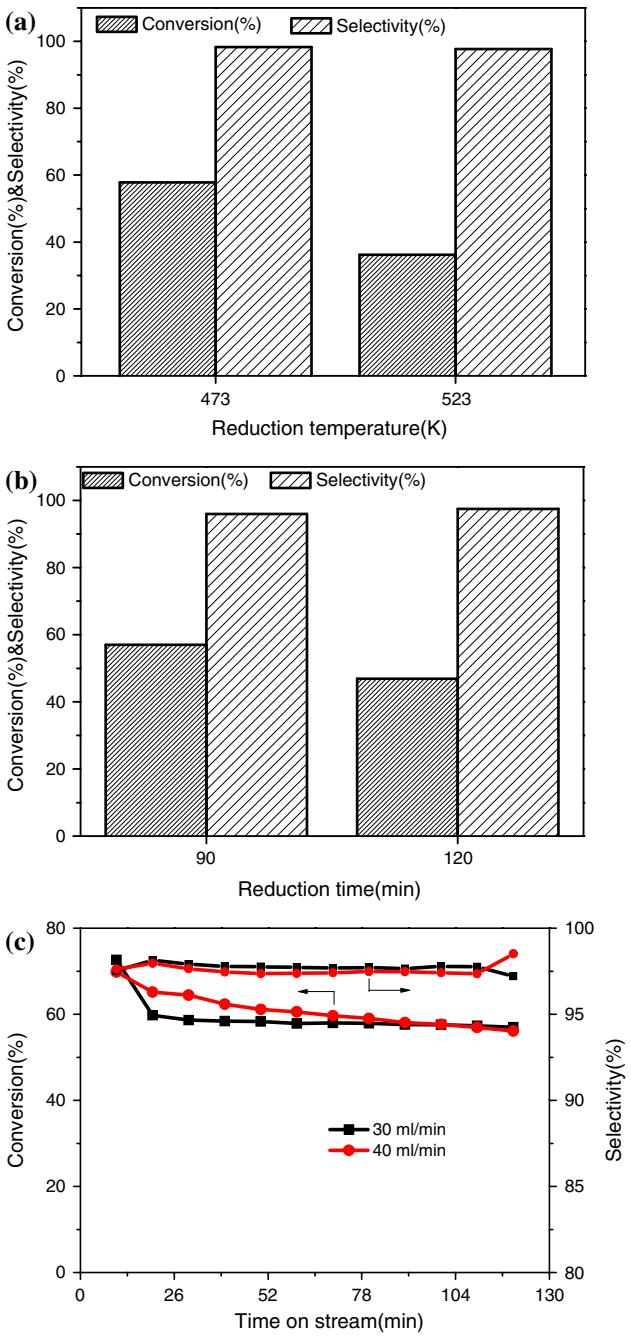

Fig. 5 Effect of depth reduction of Pt on the catalytic performance

is ready to transform to carbenium ion intermediates [28]. In the absence of Pt it is required that acid attacks directly the alkanes to form carbenium ion intermediates and much stronger acid strength is necessary. TPA is a solid superacid, but when it was supported onto the SiO_2 the acid strength decreased [8]. So we inferred that the same thing also occurred to MCM-41. When 25% TPA was impregnated onto MCM-41, the acid strength was weak and the only TPA on MCM-41 couldn't directly and efficiently transform *n*-pentane to carbenium ion intermediates.

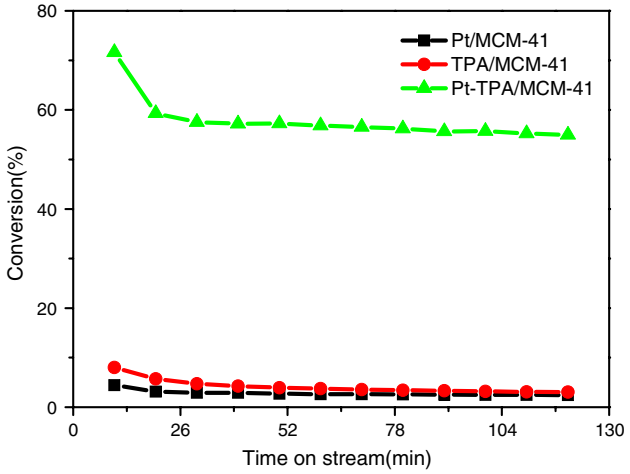

Fig. 6 Catalytic activity comparison of 2% Pt/MCM-41, 25% TPA/MCM-41, and 2% Pt-25% TPA/MCM-41

Consequently, a low catalytic activity was observed. However, as soon as the synergistic effect formed, i.e. Pt and TPA were together impregnated onto MCM-41, Pt was responsible for the formation of olefin and then the olefin on acid site isomerized. Finally a high catalytic activity was obtained.

The effect of TPA loading amount on the catalytic performance of Pt-TPA/MCM-41 is shown in Fig. 7. It is clearly that the conversions of the catalysts firstly increased with the increasing of loading amount of TPA and then decreased. A maximum conversion was obtained at 30% TPA content. This change trend is similar to that of Miyaji et al. [8, 9] reported, in which when the Pd content was constant the isomerization activities of Pd-TSA/SiO_2 also reached a maximum value with 20% TSA loading. The maximum activities corresponded to different HPAs loadings may be due to the higher surface area of MCM-41 than that of SiO_2. As this reaction can be classified as a surface reaction, the activity should be related to the amount of active acid sites on the surface. XRD patterns demonstrated that when the TPA loading amount is below 35% no characteristic diffraction peaks corresponding to TPA were observed. It is suggested that in the range of 0–30% loading TPA were well dispersed on MCM-41. Correspondingly, increasing the loading amount of TPA should enhance the amount of surface protons and further strengthen the ability of skeletal isomerization of the catalyst. Although we cannot exclude the enchanced catalytic activity arising from the interaction between surface silanol and anion of TPA which may produce stronger acidity sites for the reaction, we have no direct evidence of it. Further increase TPA loading amount leading to a decrease in conversion is probably due to the poor dispersion of TPA on MCM-41.

The role of Pt played during the course of skeletal isomerization was analyzed before. In this section the effect of Pt content on the skeletal isomerization will be introduced. Figure 8 indicates the activity and selectivity curves of catalysts with different Pt loading amount. The catalyst with 1% Pt exhibited the lowest conversion and the conversion attained to the saturation at 2% Pt. Further increase the content of Pt, no obvious change of conversion was observed. According to the analysis of the above, we know that Pt and TPA in the catalyst had a synergistic effect. So it can be inferred that the combination of 2% Pt and 30% TPA owned the optimal synergistic effect. Further increase the Pt content may improve the dehydrogenation ability of the catalyst, however no suitable active acid sites match the subsequent olefin isomerization step. From Fig. 8 we also found that the lowest conversion of catalyst demonstrated the highest selectivity consistent with the TPA addition. This result suggested that Pt probably also played some role in the cracking procedure.

The products distribution of the reaction with 2% Pt-30% TPA/MCM-41 at 473 K at the time point of 60 min are listed

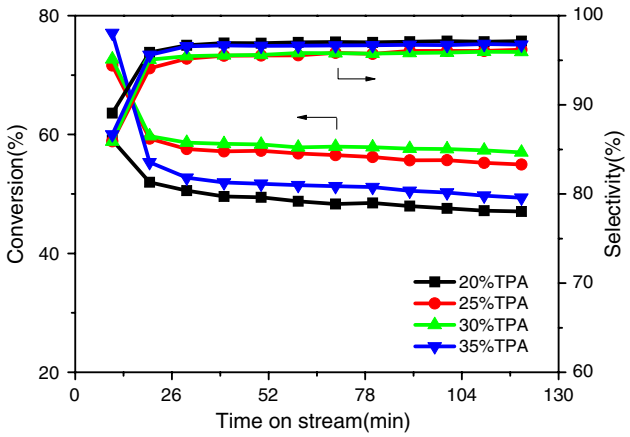

Fig. 7 Effect of different loading amount of TPA over 2% Pt/MCM-41 on the skeletal isomerization of *n*-pentane

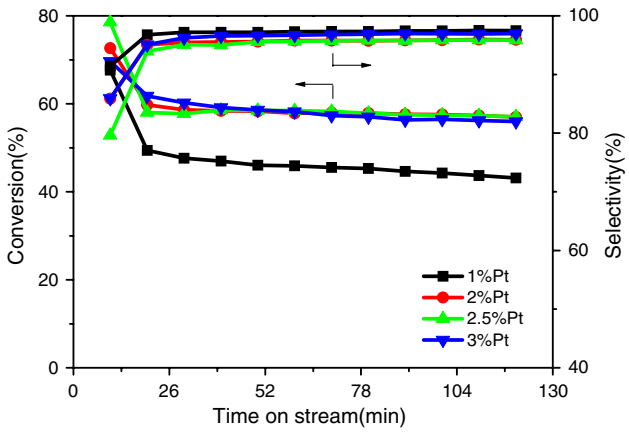

Fig. 8 Effect of different loading amount of Pt over 30% TPA/MCM-41 on the skeletal isomerization of *n*-pentane

Table 1 Product distribution of *n*-pentane skeletal isomerization over different catalysts at 473 K

Catalysts	Conversion (%)	Selectivity (%)				
		C1-C3	*i*-C4	*n*-C4	*i*-C5	C6
2% Pt-30% TPA/MCM-41	57.6	1.9	0.9	0.8	95.6	0.7

in Table 1. Iso-pentane is the principal reaction product and the by-products are methane, ethane, propane, isobutene, *n*-butane and hexanes. Usually the side reactions of isomerization of *n*-pentane are disproportion and hydrogenolysis [12]. The disproportion is a reaction of alkylation-cracking via β-scission of dimer intermediates (C10) on acid sites and produces mainly $C_3 + C_7$ and $C_4 + C_6$. However, C_6 and C_7 are more reactive and easily transformed to smaller fragments. Hydrogenolysis can convert C_5 to $C_1 + C_4$ and $C_2 + C_3$. Catalyst and reaction conditions are the principal factors to influence the side reaction type. The formation of C_6 over 2% Pt-30% TPA/MCM-41 suggested that the disproportion reaction occurred during the isomerization. From the former section, we knew that the selectivity of iso-pentane changed along with the Pt loading amount. So it can be inferred that some cracked products such as methane and ethane may form via hydrogenolysis of *n*-pentane on Pt sites. Nevertheless, the acidic properties, particularly the acid strength, are still considered to be a critical factor determining the selectivity.

From the above analysis it is clear that MCM-41supported Pt-TPA metal-acid bifunctional catalyst exhibited high skeletal isomerization activity and selectivity. In view of this, it is useful to further investigate the catalytic activity and selectivity of catalyst with different combination of noble metals, HPAs and supports. Besides TPA, TSA and MPA are another two most widely used HPAs. The influences of different HPAs on skeletal isomerization of *n*-pentane were compared in Fig. 9a. The sequence of isomerization catalytic activity is in good agreement with the acid strength order of TPA > TSA >> MPA. However, TSA exhibited the best selectivity and the selectivity of MPA as its conversion is the lowest. Although the use of TSA can improve the selectivity, its conversion is somewhat low. Because the selectivity of TPA and TSA based catalysts are close, comprehensive considering the catalytic performance, the choosing of TPA as the acid component is better. Noble metal with TPA on MCM-41 were synthesized and performed in skeletal isomerization reaction of *n*-pentane. From Fig. 9b, it can be seen that Pd promoted catalyst showed the best isomerization activity and selectivity. Obviously, Pd is the best metal active component. The sequence of the conversion of catalysts with different noble metals is Pd > Pt ≫ Ru. The skeletal isomerization

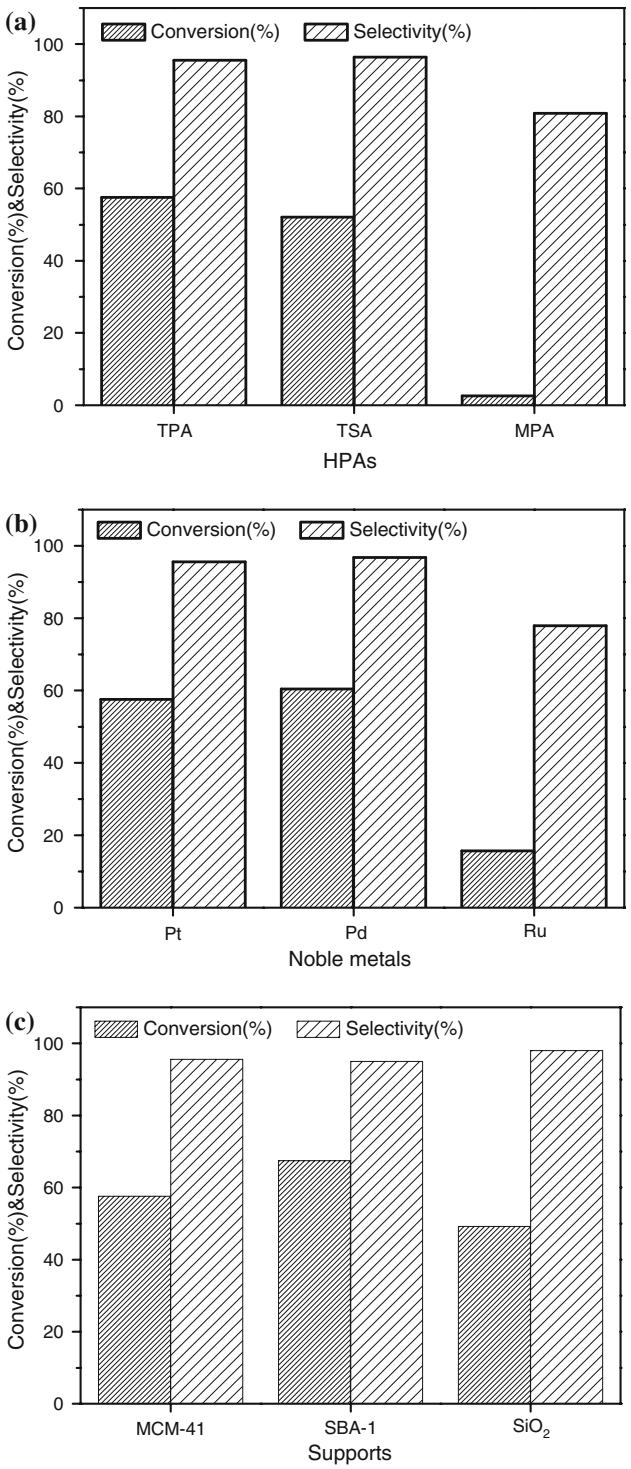

Fig. 9 Effect of catalysts with different combinations of HPAs, noble metals and supports on the skeletal isomerization of *n*-pentane

of *n*-pentane with Pt promoted TPA on different supports of MCM-41, SBA-1 and SiO_2 were carried out (see Fig. 9c). Although SBA-1 based catalyst exhibited the highest activity, SiO_2 based catalyst demonstrated the highest selectivity. The selectivity of MCM-41 and SBA-1

based catalysts are not obvious difference. As we all know, the specific surface area of SiO_2 is the lowest, so we inferred that less TPA was impregnated onto the surface of SiO_2 and of course the SiO_2 based catalyst had the weakest acid strength. As a result, the SiO_2 based catalyst had the lowest conversion and the highest selectivity. The difference of the catalytic activity of MCM-41 and SBA-1 based catalysts were considered to originate from the distinction of their pores and cages. Of course, this view of point need more experiment results to support and the related work is being done in our laboratory.

4 Conclusion

We have shown that Pt promoted TPA supported on MCM-41 is active solid acid catalyst for skeletal isomerization of *n*-pentane. For such reaction, the optimal loading amount of TPA and Pt were found to be 30% and 2%, respectively. XRD patterns showed that with the increasing of TPA loading more than 30% separate TPA crystal phase formed. However, no obvious TPA diffraction peaks were observed below 35% TPA content. Nevertheless, we still found that Keggin structure TPA present on MCM-41 when the TPA loading amount was less than 35% according to the FT-IR spectra. These results proved that TPA was finely dispersed on MCM-41 with relatively low loading amount. XPS analysis illustrated that after reduction the surface chemical oxidation states of Pt were present as Pt(0) and Pt(II). Depth reduction of the catalyst could not improve the catalytic performance. According to the cracked products distribution, the proportion of cracked products is quite low and this is typical of a monomolecular bifunctional metal-acid mechanism. The acidic properties, particularly the acid strength, are considered to be a critical factor determining the selectivity. The catalytic performance of catalysts related to different combinations with noble metals, HPAs and supports demonstrated that TPA and Pd were the optimal acid and metal components, respectively, and MCM-41 based catalysts had better catalytic performance than SiO_2 based catalyst and worse catalytic performance than SBA-1 based catalyst.

References

1. Chica A, Corma A (1999) J Catal 187:167
2. Wang W, Wang J, Chen C, Xu N, Mou C (2004) Catal Today 97:307
3. Vijay S, Wolf EE, Miller JT, Kropf AJ (2004) Appl Catal A 264:125
4. Vijay S, Wolf EE (2004) Appl Catal A 264:117
5. Li T, Wong S, Chao M, Lin H, Mou C, Cheng S (2004) Appl Catal A 261:211
6. Kuba S, Lukinskas P, Ahmad R, Jentoft FC, Grasselli RK, Gates BC, Knozinger H (2003) J Catal 219:376
7. Ivanov AV, Vasina TV, Masloboishchikova OV, Sergeeva KEG, Kustov LM, Houzvicka JI (2002) Catal Today 73:95
8. Miyaji A, Echizen T, Nagata K, Yoshinaga Y, Okuhara T (2003) J Mol Catal A 201:145
9. Miyaji A, Ohnishi R, Okuhara T (2004) Appl Catal A 262:143
10. Ivanov AV, Vasina TV, Nissenbaum VD, Kustov LM, Timofeeva MN, Houzvicka JI (2004) Appl Catal A 259:65
11. Okuhara T (2002) Catal Today 73:167
12. Liu Y, Na K, Misono M (1999) J Mol Catal A 141:145
13. Watanabe R, Suzuki T, Okuhara T (2001) Catal Today 66:123
14. Travers C, Essayem N, Delage M, Quelen S (2001) Catal Today 65:355
15. Essayem N, Taarit YB, Gayraud PY, Sapaly G, Naccache C (2001) J Catal 204:157
16. Suzuki T, Okuhara T (2001) Catal Lett 72:111
17. Kresge CT, Leonowicz ME, Roth WJ, Vartuli JC, Beck JS (1992) Nature 359:710
18. Kozhevnikov IV, Kloetstra KR, Sinnema A, Zandbergen HW, Van BH (1996) J Mol Catal A 114:287
19. Kresge CT, Marler DO, Rav GS, Rose BH, US Patent 5,366,945
20. Del Rossi KJ, Jablonski GA, Kresge CT, Kuehl GH, Marler DO, Rav GS, Rose BH, US Patent 5,475,178
21. Qian G, Lu G, Ji D, Zhao R, Qi Y, Suo J (2005) Chem Lett 34:162
22. Ji D, Ren T, Yan L, Suo J (2003) Mater Lett 57:4474
23. Beck JS, Vartuli JC, Roth WJ, Leonowicz ME, Kresge CT, Schmitt KD, Chu CTW, Olson DH, Sheppard EW, Mccullen SB, Higgins JB, Schlenkert JL (1992) J Am Chem Soc 114:10834
24. Kuang W, Rives A, Fournier M, Hubaut R (2003) Appl Catal A 250:221
25. Ji D, Zhao R, Lu G, Qian G, Yan L, Suo J (2005) Appl Catal A 281:39
26. Siahkali AG, Philippou A, Dwyer J, Anderson MW (2000) Appl Catal A 192:57
27. Geng D, Chen L, Lu G (2007) J Mol Catal A 265:42
28. Na K, Okuhara T, Misono M (1997) J Catal 170:96